

hydrazine," Rept. TR-0158(3210-10)-2, 1967, Aerospace Corp., El Segundo, Calif.

<sup>4</sup> Chang, E. T. and Gokcen, N. A., "Equilibria in  $N_2H_4$ -1, 1- $N_2H_2(CH_3)_2$  and He(or  $N_2$ )- $N_2H_4$ -1, 1- $N_2H_2(CH_3)_2$  Systems," *Journal of Physical Chemistry*, Vol. 72, 1968, pp. 2556-2562.

<sup>5</sup> Kemppinen, A. I. and Gokcen, N. A., "Density of Dibutyl Phthalate," *Journal of Physical Chemistry*, Vol. 60, 1956, pp. 126-127.

<sup>6</sup> Seidell, A. and Linke, W. F., *Solubilities of Inorganic and Metal Organic Compounds*, Van Nostrand, New York, 1958.

<sup>7</sup> Penner, S. S., *Chemistry Problems in Jet Propulsion*, Pergamon Press, New York, 1957, Ch. XII.

<sup>8</sup> Hildebrand, J. H. and Scott, R. L., *Regular Solutions*, Prentice-Hall, Englewood Cliffs, N.J., 1962, p. 47.

<sup>9</sup> Hirschfelder, J. O., Curtiss, C. F., and Bird, R. B., *Molecular Theory of Gases and Liquids*, Wiley, New York, 1964, pp. 156, 191, and 195; also p. 44 in Ref. 8.

<sup>10</sup> Stephen, H. and Stephen, T., eds., *Solubilities of Inorganic and Organic Compounds*, MacMillan, New York, 1963.

<sup>11</sup> Chang, E. T. and Gokcen, N. A., "Rate of Solution of  $N_2$  in Liquid  $N_2O_4$ ," Rept. TR-1001 (2210-10)-1, 1966, Aerospace Corp., El Segundo, Calif.

## Graphically Determining Sounding Rocket Vehicle Attitudes

CHARLES F. MILLER JR.\*

Goddard Space Flight Center, Greenbelt, Md.

**C**OORDINATES used to determine the attitude of a sounding rocket vehicle are commonly derived from the solar or lunar aspect angle, designated  $\alpha$ , in association with the magnetic aspect angle, designated  $\theta$ , which is the angle of the rocket's longitudinal axis with respect to the local magnetic field vector. On sounding rockets, optical sensors measure  $\alpha$  once each spin cycle, and a flux-gate magnetometer measures  $\theta$ . The angle between  $\alpha$  and  $\theta$ , designated the phase angle  $\phi$ , is measurable from telemetry records. Sun and magnetic south point positions are plotted; then  $\alpha$  and  $\theta$  are used to determine the azimuth and zenith distance of the rocket's longitudinal axis. When the time sequence of rocket positions in flight has been plotted, the momentum vector can be determined. With any known rocket position,

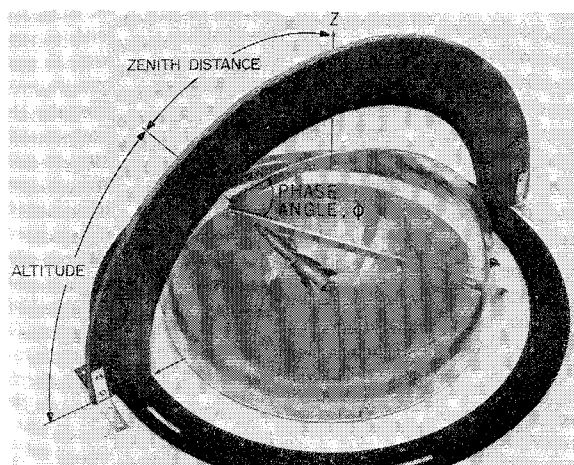


Fig. 1 Aspect-angle protractors aligned with sun and magnetic south point, and generating phase angle at the rocket.

any other portion of the sky can be mapped for that orientation, using coordinate transformation.

Figure 1 depicts the three-dimensional parameters. The altitude  $A$  of the rocket is the number of degrees (0-90) on the vertical circle from the horizon to the axis of the rocket. The zenith distance is the angle between the zenith  $Z$ , directly over the center of gravity of the rocket, and the longitudinal axis of the vehicle. The zenith distance is the complement of the altitude and, in this discussion, is represented by the arc at a fixed radius from the origin. The sky is represented by a spherical shell on which lines of altitude and azimuth are plotted every  $10^\circ$ . The rocket's attitude is the combination of its altitude and its azimuth. On this shell, the position of the vehicle's nose, or the position of any celestial body, can be plotted. The rocket's center of mass locates the center of the base of the plastic hemisphere; from that point  $\alpha$ ,  $\theta$ , and  $\phi$  are measured. In Fig. 1, a hinged protractor, concentric with the rocket's center of mass, is situated with the hinge aligned with the rocket's longitudinal axis, one leg in the plane of the incident sunlight, and the other in the plane of the magnetic flux vector, i.e., over the south magnetic point. The phase angle  $\phi$  can be measured between the protractor's two halves and can be seen to be the dihedral angle between two planes, one made by the angle of the sun's rays with the rocket's longitudinal axis and the other made by the angle of the local magnetic flux vector with that axis.

Figure 2 is a zenith view of the same situation, with black arcs defining  $\alpha$  and  $\theta$ . From the magnetic south point to the sun, a black arc completes the spherical triangle used to determine the zenith distance and azimuth of the vehicle's nose. As a step toward reducing the three-dimensional system to two dimensions, Fig. 2 was taken directly over the zenith. Thus, the view represents the projection of the horizon system down to the plane of the horizon. The altitude is a cosine function of the radius from  $Z$ , thus the first  $15^\circ$  of altitude are hardly separable in the photograph.

### Reduction to Polar Coordinates

To transform spherical parameters to two coordinates, a plot is made on polar graph paper of the sky from the horizon to the zenith. In Fig. 3, such a plot has been made of the situation depicted in Fig. 2. In Fig. 3, any radius is an azimuth angle  $R$  with reference to north, and increments along a chosen radius mark either the altitude or its complement, the zenith distance. The time, latitude  $\beta$ , and longitude  $\lambda$  of the rocket flight are required for the location of the sun on polar graph paper. For Nike-Apache shots, an average solar position is within the required accuracy, but for longer and higher flights, the trajectory should be divided into parts, and each successive time interval should specify  $\beta$  and  $\lambda$  to

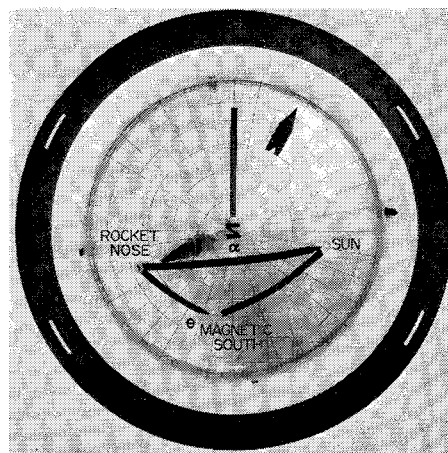


Fig. 2 Zenith view of Fig. 1, showing spherical triangle.

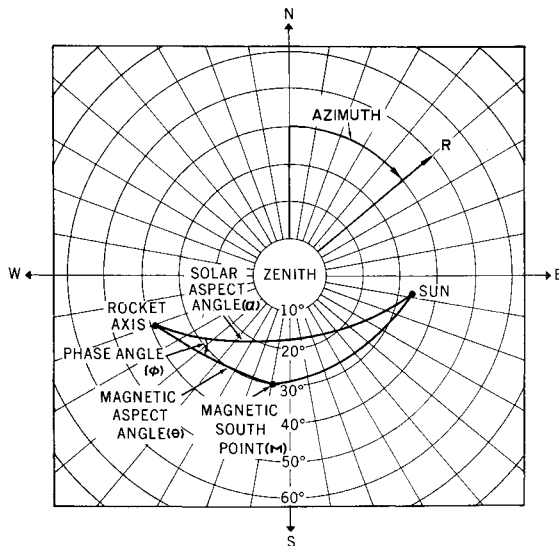


Fig. 3 A plot of Fig. 2 on plane polar paper.

find the sun's altitude and azimuth. A large variety of celestial navigational techniques can be used to find the sun's altitude and azimuth; the reference at the end of this discussion mentions the source of methods this writer has found to be best. The magnetic south point, or flux vector, can be found as a function of  $\beta$ ,  $\lambda$ , and the altitude above the ground.

In Fig. 2,  $R$  is  $249^\circ$  and  $A$  is  $52^\circ$ . The azimuth of the sun is  $98^\circ$  and its altitude is  $56^\circ$ . The magnetic flux vector for White Sands Missile Range (WSMR) is marked  $M$ ; it has an azimuth of  $192^\circ$  and an altitude of  $60^\circ$ . The zenith  $Z$  is directly over the center of gravity of the rocket. All coordinates of Fig. 2 have been transferred to identical positions in Fig. 3. Translucent paper is used, to permit viewing in combination with other transparencies.

If concentric circles are drawn, in Fig. 2, on the plastic hemisphere about the sun's  $0^\circ$  aspect angle point  $S$ , then these circles will represent lines of equal solar aspect angle. If a zenith view is presented of the plot of such circles, they will appear as skewed ellipses. A rocket pointing at any one of these ellipses will have that solar aspect angle. Similarly, equal magnetic aspect lines can be plotted, in zenith view, as skewed ellipses. In Fig. 4, solar and magnetic aspect-angle ellipses have been superimposed on the polar coordinate system of Fig. 3. (This technique is further discussed in Ref. 1.) The superimposed solar aspect circles are incomplete ellipses of the solar aspect angles for a sun altitude of  $56^\circ$ , indicated as  $(+S)$ ; the superimposed magnetic aspect lines are for WSMR, for which the magnetic flux vector  $+M$  has an altitude of  $60^\circ$  and an azimuth of  $192^\circ$ . Figure 4 depicts the conditions under which Nike-Apache, Flight 14.363 GT was fired: azimuth of the sun was  $98^\circ$  and the magnetic flux vector was as outlined above for WSMR.

At this particular instant in the rocket's flight, the solar and magnetic aspect angles were  $41^\circ$  and  $39^\circ$ , respectively. From Fig. 4, the altitude of the vehicle is seen to be  $80^\circ$  ( $10^\circ$  zenith distance) and the azimuth is  $330^\circ$ . The combination of altitude and azimuth make up the attitude of the vehicle. The two phase lines drawn from the solar and magnetic transparencies thus show an angle of  $75^\circ$ .

Instead of using telemetered  $\alpha$  and  $\theta$ , an alternate method shown in Fig. 5 is based on telemetered  $\alpha$  and  $\phi$ . In Fig. 5, a  $45^\circ$  transparency (corresponding to the median rocket attitude at the telemetered  $\alpha$  of  $79^\circ$ ) has been placed with its center on the line representing the  $79^\circ$  aspect-angle line with respect to the sun. Since  $\theta$  has also been telemetered ( $39^\circ$ , in this case), the transparency can be moved along the  $79^\circ$  ellipse until the phase angle between the sun and the

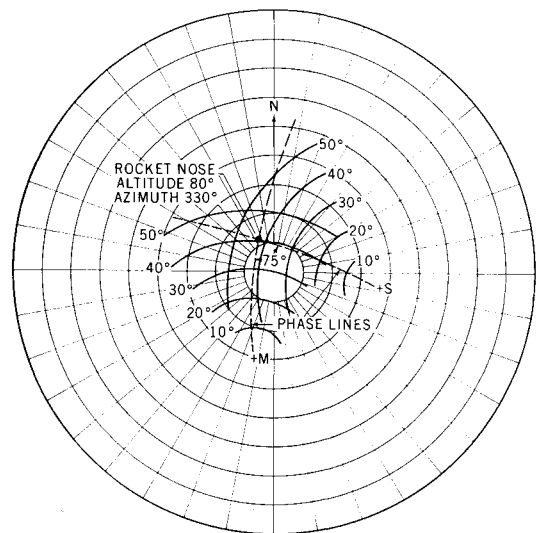


Fig. 4 Superposition of partial solar and magnetic aspect-angle (skewed ellipses) transparencies on Fig. 3 to derive the values of rocket altitude, azimuth, and phase angle.

magnetic south point becomes correct ( $39^\circ$ ). Care must be taken that the  $45^\circ$  transparency does not move into the  $35^\circ$  or  $55^\circ$  areas. The "radial" lines in the  $45^\circ$  transparency are two-dimensional plots of great circles on the original three-dimensional sky model. (These radial lines, if employed with transparencies such as those of Fig. 3, constitute legs of  $\phi$  between  $\alpha$  and  $\theta$ .)

This graphic method works equally well with the celestial coordinate system.<sup>1</sup> The system is geocentric, its coordinates are declination, right ascension, and sidereal hour angle. The zenith is replaced by true north, altitude is replaced by declination, and azimuth is replaced by either sidereal hour angle or right ascension. In this system, the coordinates can be taken directly from a star almanac.

#### Analysis of a Rocket Flight

Nike-Apache Flight 14.363 GT was fired from White Sands Missile Range on June 4, 1968 and reached an apogee of 130 km. It was noted that from 70 sec after liftoff to 244.75 sec,  $\alpha$  varied sinusoidally from  $38.5^\circ$  to  $45.0^\circ$  at a constant period, and from 244.75 sec until atmosphere re-entry it varied from  $27^\circ$  to  $94^\circ$  by another constant period.

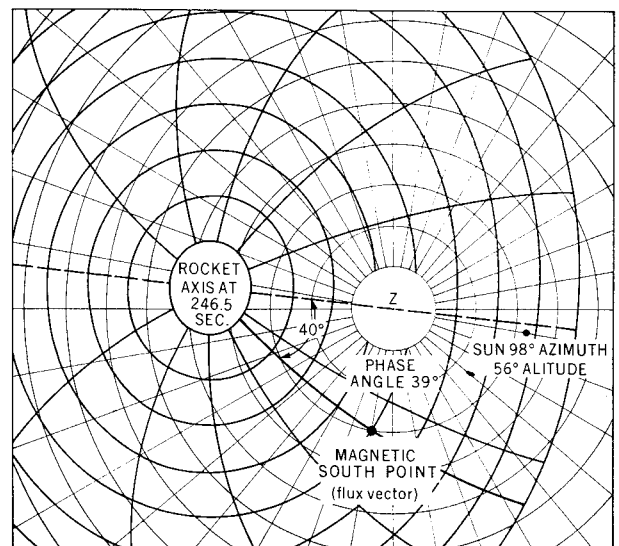


Fig. 5 Transparency placed over rocket axis so that the sky can be mapped relative to the rocket.

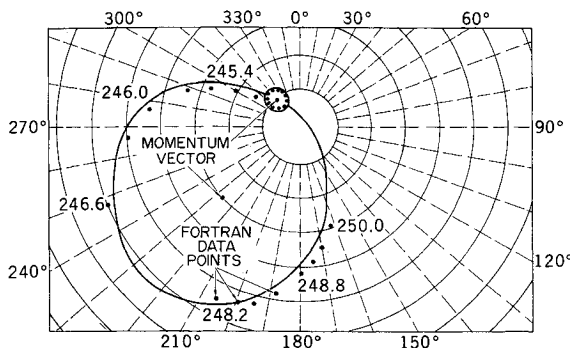


Fig. 6 Comparison of graphic method (with solid lines) showing coning and FORTRAN corroborations (dots).

The value of  $\theta$  varied from maximum to minimum in precisely the same time periods. The spin of the vehicle was measured using the  $\alpha$  signal during early and late flight and was found to be a constant 9.09 cps. The  $\alpha$  signals more precisely define the spin time than the lateral  $\theta$  signals. The total angular momentum of the vehicle is divided between the spin and cone periods, and a change in one means a change in the other, for a constant mass in space. From 70 sec to 245 sec, the variation in  $\alpha$  is sinusoidal. A phase relationship with the maximum and minimum  $\theta$ 's was established, and, by plotting these positions, it was found that the vehicle coned six times about a momentum vector of altitude  $80^\circ$  and azimuth  $320^\circ$ . The cone angle was  $6.5^\circ$  and the period was 32.72 sec.

From 20 to 95 sec, the change in latitude and longitude indicated, through the radar plots, the velocity vector. The velocity vector during the powered portion of the flight is the average attitude of the vehicle. From this portion of the flight, the phase angle between the sun and magnetic south point was checked. This confirms the placement of the  $\alpha$  sensors and the magnetometers within the payload.

At 244.75 sec (Fig. 6) the second stage separated from the payload and  $\alpha$  began to vary sinusoidally from  $27^\circ$  to  $94^\circ$ . The period of the new large cone was found to be 6.25 sec, and the coning angle was  $\sim 67^\circ$  about a new momentum vector. The new momentum vector's altitude was  $60^\circ$ , and its azimuth was  $229^\circ$ . It coned 10 times about this new vector before re-entry into the atmosphere.

At 259 sec, 51 solar signals were counted on the telemetry record, as were 50 magnetic aspect maximum signals on the lateral magnetometer. It was noted that the former coincided with the latter. One magnetometer maximum signal was lost because the vehicle coned once around the magnetic south point in the same interval. In the manner of Fig. 4, positions were plotted for the solar and magnetic aspect angles for both early and late flight (Fig. 6). The two skewed ellipses in Fig. 6 represent the epicycloidal motion immediately before and after ejection of the second stage and the consequent change in the momentum vector.

In Fig. 5, the  $45^\circ$  transparency (corresponding to the rocket's altitude) has been placed with its center directly over the nose position at 246 sec after liftoff. At this time, the rocket's altitude is about  $45^\circ$  and the azimuth is  $276^\circ$ . The rest of the sky, seen from the rocket nose, was then mapped by this transparency, and the aspect angle at the vehicle and the azimuth and altitude of any other celestial body can be plotted.

Figure 6 also compares the values from the FORTRAN analysis and data from the graphic analysis. Agreement is within  $2^\circ$ .

#### Reference

- 1 Miller, C. F., Jr., "A Graphic Method for Determining the Absolute Attitude of Sounding Rocket Vehicles," TN D-5172, May 1969, NASA.

## Heat Conduction through Fins with Nonadiabatic Tips

Y. S. Lou\*

University of Delaware, Newark, Del.

#### Nomenclature

$h$	= convective film coefficient
$k$	= thermal conductivity
$L$	= length of longitudinal fin
$L_c$	= corrected length of a longitudinal fin
$N$	= $(hp/ks)^{1/2}$
$p$	= surface area per unit width of fin
$q$	= heat flux
$r$	= radius
$r_{2c}$	= corrected outer radius of a radial fin
$s$	= cross-sectional area per unit width of fin
$T, T_f$	= temperature, and temperature of ambient fluid
$\delta$	= half-thickness of fin
$\epsilon$	= length of extended tip
$\theta$	= $T - T_f$
$I_0, K_0$	= zeroth-order modified Bessel functions of the first and second kinds

#### Introduction

**F**INS are commonly used in many heat exchanger applications. Fin geometries are diverse and are selected on the basis of efficient performance, minimum weight, and ease of manufacture. For those cases where the heat transfer from the fin tip is negligible, the adiabatic boundary condition facilitates obtaining exact solutions. However, in many cases the fin tip is not adiabatic, yielding a boundary condition quite involved for all but simple fin geometries. Harper and Brown<sup>1</sup> proposed an approximation technique for such cases, in which an imaginary extension is added to the fin tip. The temperature of the extension is assumed constant, and the heat flow from the end of the actual fin is dissipated through the two sides of the extension, such that the end of the imaginary tip is adiabatic. They approximate the length  $\epsilon$  of the extension as one-half the actual thickness of the fin. When compared to the exact solution, this approximation is not accurate for certain combinations of fin geometry and operating conditions.<sup>2</sup>

This Note presents a method for calculating the length  $\epsilon$  by treating the imaginary extension as a fin with an adiabatic tip, such that the heat flow at the base of the extension equals the heat loss from the tip of the actual fin. In this manner, variable temperature is allowed in the extension, and  $\epsilon$  can be calculated directly. Theoretically, the new method should lead to exact solutions for predicting the heat conduction rate. We shall illustrate the method for both longitudinal and radial fins of constant thickness. For simplicity, the following assumptions shall be made in both cases: steady-state operation, uniform thermal conductivity ( $k = \text{const}$ ), uniform convective film coefficient ( $h = \text{const}$ ), one-dimensional temperature distribution, i.e.,  $k/h\delta \gg 1$ , and uniform fluid temperature ( $T_f = \text{const}$ ).

#### Description of the Problem

##### Case A: Longitudinal fin of constant thickness

Consider a fin of length  $L$  and thickness  $2\delta$  used to transfer heat from a body at uniform temperature  $T_0$  (Fig. 1). Taking a small element  $\Delta x$ , a heat balance in the  $x$  direction is

$$sk \frac{\partial T}{\partial x} - \left[ sk \frac{\partial T}{\partial x} + \frac{\partial}{\partial x} \left( ks \frac{\partial T}{\partial x} \right) \Delta x \right] - hp(T - T_f)\Delta x = 0 \quad (1)$$

Received May 21, 1969.

\* Assistant Professor, Department of Mechanical and Aerospace Engineering. Member AIAA.